CFD Letters

Journal homepage:
https://semarakilmu.com.my/journals/index.php/CFD_Letters/index
ISSN: 2180-1363

The Velocity, Temperature and Concentration Profiles for Triple Diffusive Casson Fluid Flow Subjected to the Soret-Dufour Parameters

Siti Suzilliana Putri Mohamed Isa[1,2,*], Nanthini Balakrishnan[1], Nurul Syuhada Ismail[3], Norihan Md. Arifin[1,4], Fadzilah Md Ali[1,4]

[1] Institute for Mathematical Research, Universiti Putra Malaysia, 43400 UPM Serdang, Selangor Darul Ehsan, Malaysia
[2] Centre of Foundation Studies for Agricultural Science, Universiti Putra Malaysia, 43400 UPM Serdang, Selangor Darul Ehsan, Malaysia
[3] Centre for Pre – University Studies, Universiti Malaysia Sarawak, 94300, Kota Samarahan, Sarawak, Malaysia
[4] Department of Mathematics, Faculty of Science, Universiti Putra Malaysia, 43400 UPM Serdang, Selangor Darul Ehsan, Malaysia

ARTICLE INFO

Article history:
Received 22 June 2023
Received in revised form 21 July 2023
Accepted 25 August 2023
Available online 12 December 2023

Keywords:
Triple diffusive; Casson fluid; Soret-Dufour

ABSTRACT

The triple-diffusive convection with the involvement of non-Newtonian fluid has many applications in the science and technology field, industrial processes, and also in research works. Therefore, the mathematical model of the triple-diffusive convection of Casson fluid by the mathematical approach is investigated. In addition, a mathematical model for the triple-diffusive convection of Casson fluid flow beyond a nonlinear compressing sheet has been formulated and solved by numerical approach, where this is the main objective of this study. This model is subjected to mass transfer and heat transfer, known as Soret and Dufour effect (Soret-Dufour). The Soret effect is occurred when the temperature gradient is produced, whereas the differences in mass cause the Dufour effect. The model is formed by the continuity equation, momentum equation, energy equation, and concentration equations of component 1 and 2, together with the boundary conditions. They have been reduced to ordinary differential equations, and subsequently, they have been implemented in bvp4c programme provided by MATLAB software to get the numerical solutions. The solutions obtained were profiles of velocity, temperature and concentration of both components. Next, the effect of Casson parameter, Soret parameter, and Dufour parameter have been investigated by changing their values of inside the coding in MATLAB and observing the behaviour of the related profiles due to these parameters. The main results from this study were: The velocity of the Casson fluid reduced as the Casson parameter enhanced, increment in both Soret and Dufour parameters caused the temperature to decrease, and the fluid concentration was higher for the increasing Soret number.

1. Introduction

The convective flow of non-Newtonian fluid plays vital role in industries, chemical engineering and also in many biological processes. Due to undeniable applications in medical field, metallurgy, and chemical engineering, non-Newtonian Casson fluid is being reported by many researchers

* *Corresponding author.*
E-mail address: ctsuzilliana@upm.edu.my (Siti Suzilliana Putri Mohamed Isa)

https://doi.org/10.37934/cfdl.16.3.1527

recently. Meanwhile, the fluid flow induced by a compressing or extending sheet is highly related to many technological processes. Pramanik [1] studied the characteristic of a pseudo-plastic liquid owned by Casson fluid. When the rate of shear is zero, Casson fluid is assumed to have viscosity which is infinity. Contrastly, when the rate of shear is infinity, the viscosity becomes zero. The Casson fluid bounded by an extending sheet have been reported due to the additional impacts such as magnetic field [2-4], chemical reaction [2], viscous dissipation [2], various thermal conductivity [2], Soret-Dufour [3], internal heat generation [5] and so on. The pioneer publication of the numerical analysis on the Casson fluid flow bounded by a compressing sheet is authored by Bhattacharyya [6]. The recent studies due to the Casson fluid flow beyond the compressing or extending sheet are published with the details mathematical analysis [7-14].

Double-diffusive convection is induced when the there are when there is a significant difference between two values of the temperature and concentration distributions [15]. This type of convection is crucial in areas like oceanography [16]. Hence, many researchers have studied the involvement of double-diffusive convection in the fluid flow induced by extending/compressing sheet. In 2017, the free double-diffusive convection and mixed double-diffusive convection are considered by Kumar *et al.,* [16] and Patil *et al.,* [17], respectively. The effects of heat and mass transfer on the mixed double-diffusive convection have been considered for the various types of fluid: Newtonian [18, 19], Maxwell [20, 21], and Casson [8, 9].

Triple-diffusive convection is the fluid flow in which the density depends on three diffusive components with no similar properties (thermal diffusion and dual species/components diffusion). The supreme utilization of this type of convection can be seen in warming of stratosphere [22]. Researchers are starting to pay attention to this convection as this is the first step in order to explore convection with more than three components. The experimental study of the triple-diffusive convection is performed by saturating a porous horizontal layer with the fluid mixture, heating the mixture from below and adding salt from above and below [23]. The triple-diffusive convection in a nanofluid over an extending sheet with nonlinear velocity was studied by Goyal and Bhargava [24]. Subsequently, the numerical study of the triple-diffusive convection in a Casson fluid and Eyring-Powell nanofluid over an extending sheet was reported by Archana *et al.,* [25] and Khan *et al.,* [26], respectively.

Based on the previous studies as above, there is no publications for the fluid flow over a compressing sheet for the case of triple-diffusive flow. The ultimate goal of this study is to solve a mathematical model of the triple diffusive Casson fluid flow over a nonlinear compressing sheet subjected to the Soret-Dufour effects. Thermo-diffusion or Soret effect is defined as the transfer of mass created by the temperature difference. Besides, the diffusion-thermo or Dufour effect shows the occurrence of heat transfer process due to mass difference.

2. Methodology

The incompressible Casson fluid flow through a horizontal compressing sheet is considered to be steady, laminar and free convection. The mathematical formulation in this study, is extended from Archana *et al.,* [25] from the case of horizontal flat sheet to the new case: compressing flat sheet. The Casson fluid contains two different components with no similar properties. The mixture of these components in the fluid are assumed to be homogeneous and is in local thermal equilibrium. Component 1 and component 2 having different concentrations C_1 and C_2 respectively. Since the temperature at surface varies from temperature of surrounding air, Oberbecke-Boussinesq approximation is applied. The graphical ilustration of this problem is presented in Figure 1. From Figure 1, the compressing sheet is inclined with an angle of ω from the fixed vertical axis. The velocity

in $x-$ and $y-$ axes is denoted by u and v. The velocity in the direction of shrinking sheet is represented by u_w whereas $v_w < 0$ is the wall mass suction velocity. The gravitational acceleration is denoted as g. In addition, T_w, C_{1w} and C_{2w} refers to the constant values of temperature, solutal concentration of component 1 and component 2 respectively. The ambient temperature and solutal concentrations are represented by T_∞, $C_{1\infty}$ and $C_{2\infty}$. The constant values with subscript w is assumed to be higher than the other constants with subscript ∞. Based on the aforementioned assumptions, the governing equations are presented in Eq. (1) – Eq. (5).

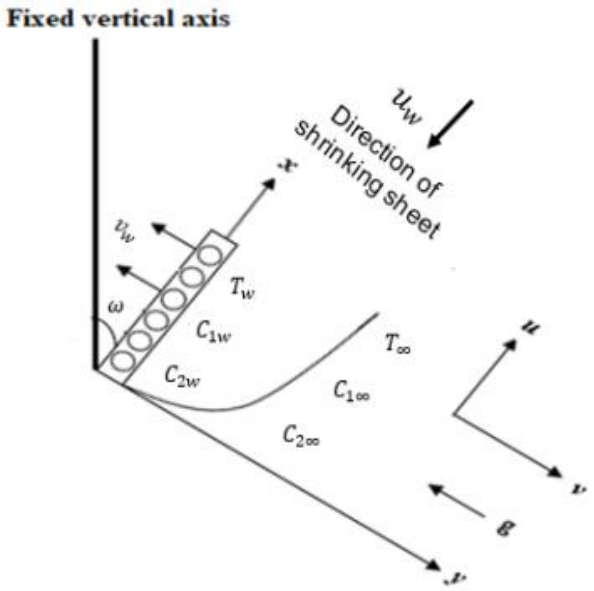

Fig. 1. The illustration of the model problem

$$u_x + u_y = 0 \tag{1}$$

$$\rho_f\left(uu_x + vu_y\right) = \mu\left(1 + \frac{1}{\beta}\right)u_{yy} - \left\{(1 - C_\infty)\rho_{f\infty}\begin{bmatrix}\beta_T(T - T_\infty) + \beta_{C1}(C_1 - C_{1\infty}) \\ +\beta_{C2}(C_2 - C_{2\infty})\end{bmatrix}\cos\omega\right\}g \tag{2}$$

$$uT_x + vT_y = \alpha T_{yy} + \tau\left[\frac{D_T}{T_\infty}\left(T_y\right)^2\right] - \frac{1}{(\rho c)_f}(q_r)_y + D_{TC1}(C_1)_{yy} + D_{TC2}(C_2)_{yy} \tag{3}$$

$$u(C_1)_x + v(C_1)_y = D_{s1}(C_1)_{yy} + D_{C1T}T_{yy} \tag{4}$$

$$u(C_2)_x + v(C_2)_y = D_{s2}(C_2)_{yy} + D_{C2T}T_{yy} \tag{5}$$

The symbols occurred in the equations above are as follow: ρ_f is the fluid density, μ is the fluid viscosity coefficient, β is the Casson parameter, β_T is the coefficient of thermal expansion, β_C is the coefficient of volumetric solutal expansion of component 1 and component 2 respectively, $\alpha = k/(\rho c)_f$ is the thermal diffusivity of the fluid, k is the thermal conductivity, c_f is the specific heat coefficient of fluid, $\tau = (\rho c)_p/(\rho c)_f$ is the ratio of effective heat capacity of the nanoparticle material to heat capacity of the fluid, D_T is the coefficient of thermophoretic diffusion, q_r is the radiative heat flux, D_{TC} and D_{CT} are the Dufour and Soret type of diffusivity, and D_S is the solutal

diffusivity. The subscripts 1 and 2 occurred in the certain symbols are referred to the components 1 and 2, respectively. The current flow analysis has the following boundary conditions:

$$\begin{aligned} &u = \lambda\alpha A^{1/2}x^{1/2}, \quad v = v_w, \quad T = T_w, \quad C_1 = C_{1w}, \quad C_2 = C_{2w} \quad \text{at} \quad y = 0, \\ &u \to 0, \qquad\qquad v \to 0, \quad T \to T_\infty, \quad C_1 \to C_{1\infty}, \quad C_2 \to C_{2\infty} \quad \text{as} \quad y \to \infty. \end{aligned} \tag{6}$$

where $\lambda < 0$ is the shrinking parameter.

The dimensionless similarity variables as below:

$$\begin{aligned} &\psi = \alpha {R_{ax}}^{1/4}, \quad u = \psi_y, \quad v = -\psi_x, \quad R_{ax} = \frac{g(1-C_\infty)\beta_T(T_w-T_\infty)x^3}{\nu\alpha}, \\ &\eta = {R_{ax}}^{1/4}\frac{y}{x}, \quad T = T_\infty[1 + (\theta_w - 1)\theta(\eta)], \\ &\theta(\eta) = \frac{T-T_\infty}{T_w-T_\infty}, \quad \phi_1(\eta) = \frac{C_1-C_{1\infty}}{C_{1w}-C_{1\infty}}, \quad \phi_2(\eta) = \frac{C_2-C_{2\infty}}{C_{2w}-C_{2\infty}}, \end{aligned} \tag{7}$$

where ψ is the stream function for the flow in which by differentiating with respect to x and y we will get the velocity components u and v, R_{ax} is the Rayleigh's number, η is the boundary layer thickness, $\theta_w = T_w/T_\infty$ where θ_w >1 is the ratio of temperature, θ refers to the temperature profile, ϕ_1 and ϕ_2 refers to the concentration profile of component 1 and component 2 respectively. Finally, Eq. (1) – Eq. (6) are transformed into Eq. (8) – Eq. (12) by implementing Eq. (7).

$$\left(1 + \frac{1}{\beta}\right) f_{\eta\eta\eta} + \frac{1}{4Pr}\left(3ff_{\eta\eta} - 2\left(f_\eta\right)^2\right) - (\theta + N_{C1}\varphi_1 + N_{C2}\varphi_2)\cos\omega = 0 \tag{8}$$

$$\begin{aligned} &\{1 + Rd[1 + (\theta_w - 1)\theta]^3\}\theta_{\eta\eta} + \frac{3}{4}\theta_\eta f + N_t\left(\theta_\eta\right)^2 + Db_1(\varphi_1)_{\eta\eta} + Db_2(\varphi_2)_{\eta\eta} \\ &+3Rd[1 + (\theta_w - 1)\theta]^2(\theta_w - 1)\left(\theta_\eta\right)^2 = 0 \end{aligned} \tag{9}$$

$$\phi_{1_{\eta\eta}} + \frac{3}{4}Le_1 f\phi_{1_\eta} + Sr_1\theta_{\eta\eta} = 0 \tag{10}$$

$$\phi_{2_{\eta\eta}} + \frac{3}{4}Le_2 f\phi_{2_\eta} + Sr_2\theta_{\eta\eta} = 0 \tag{11}$$

$$\begin{aligned} &f_\eta = \lambda, \quad f = S, \quad \theta(0) = 1, \quad \varphi_1(0) = 1, \quad \varphi_2(0) = 1 \quad \text{at} \quad \eta = 0, \\ &f_\eta \to 0, \quad f \to 0, \quad \theta(\infty) \to 0, \quad \varphi_1(\infty) \to 0, \quad \varphi_2(\infty) \to 0 \quad \text{as} \quad \eta \to \infty. \end{aligned} \tag{12}$$

where the subscript η is the differentiation with respect to boundary layer thickness η. The physical parameters occurred in Eq. (8) – Eq. (12) are tabulated in Table 1. In this table, σ^* refers to the Stefan-Boltzmann constant and k^* refers to the mean absorption coefficient.

The final stage of methodology is by performing numerical calculation on the Eq. (8) – Eq. (12) using MatLab bvp4c program. The graphical illustrations are subjected to the increasing Casson, Soret, and Dufour parameters. The related Eq. (8) – Eq. (12) are transformed into the initial value problem.

2.1 Verification Method

The numerical solutions obtained from MatLab bvp4c coding are compared with another type of numerical method, namely as shooting method. This method is developed in Maple software, which

provides the solutions for the boundary value problems.The numerical findings of boundary layer flow by implementing shooting method have been reported [27, 28]. Therefore, the following equations are introduced:

$f_\eta = fp,$

$fp_\eta = fpp,$

$$fpp_\eta = \frac{-\left[\frac{1}{4Pr}(3ffpp-2(fp)^2)-(\theta+N_{C1}\phi_1+N_{C2}\varphi_2)\cos\omega=0\right]}{\left(1+\frac{1}{\beta}\right)} \tag{13}$$

$\theta_\eta = \theta p,$

$$\theta p_\eta = \frac{-\left[\begin{matrix}\frac{3}{4}\theta pf+N_t(\theta p)^2-\frac{3}{4}Db_1[Le_1 f\phi_1 p]-\frac{3}{4}Db_2[Le_2 f\phi_2 p] \\ +3Rd[1+(\theta_w-1)\theta]^2(\theta_w-1)(\theta p)^2\end{matrix}\right]}{1+Rd[1+(\theta_w-1)\theta]^3-\frac{3}{4}Db_1 Sr_1} \tag{14}$$

$\phi_{1_\eta} = \phi_1 p,$

$$\phi_1 p_\eta = -\frac{3}{4}\left[Le_1 f\phi_1 p - Sr_1\frac{\left[\begin{matrix}\frac{3}{4}\theta pf+N_t(\theta p)^2-\frac{3}{4}Db_1[Le_1 f\phi_1 p]-\frac{3}{4}Db_2[Le_2 f\phi_2 p] \\ +3Rd[1+(\theta_w-1)\theta]^2(\theta_w-1)(\theta p)^2\end{matrix}\right]}{1+Rd[1+(\theta_w-1)\theta]^3-\frac{3}{4}Db_1 Sr_1}\right] \tag{15}$$

$\phi_{2_\eta} = \phi_2 p,$

$$\phi_2 p_\eta = -\frac{3}{4}\left[Le_2 f\phi_2 p - Sr_2\frac{\left[\begin{matrix}\frac{3}{4}\theta pf+N_t(\theta p)^2-\frac{3}{4}Db_1[Le_1 f\phi_1 p]-\frac{3}{4}Db_2[Le_2 f\phi_2 p] \\ +3Rd[1+(\theta_w-1)\theta]^2(\theta_w-1)(\theta p)^2\end{matrix}\right]}{1+Rd[1+(\theta_w-1)\theta]^3-\frac{3}{4}Db_1 Sr_1}\right] \tag{16}$$

$$fp=\lambda, \quad f=S, \quad \theta=1, \quad \phi_1=1, \quad \phi_2=1 \quad \text{at} \quad \eta=0, \tag{17}$$

$$fp\to 0, \quad f\to 0, \quad \theta\to 0, \quad \phi_1\to 0, \quad \phi_2\to 0 \quad \text{as} \quad \eta\to\infty.$$

In the step of verification method, the guess value for $f_{\eta\eta}, -\theta_\eta, \ -\phi_{1_\eta}$ and $-\phi_{2_\eta}$ have to be predicted in this method, together with the guess value of highest boundary layer thickness η_∞ . The final numerical results are obtained when the most appropriate value of η_∞ is selected and until two consecutive values of $f_{\eta\eta}(0), -\theta_\eta(0), -\phi_{1_\eta}(0)$ and $-\phi_{2_\eta}(0)$ vary significantly by a specified values. The comparison between Matlab bvp4c and shooting method is presented in Table 2 for the first solution, and these values show good agreement. The first numerical solutions for the dual solutions are proved to be the most stable and reliable result [20, 21]. These results are obtained under the conditions of these values: $\omega = 80°$, $\mathrm{Pr} = 1$, N_{C1}=0.1, N_{C2}=0.5, $N_t = 0.1$, Db_1 =0.2, Db_2 =1.0, $Le_1 = 0.5$, $Le_2 = 0.7$, Rd=0.05, θ_w=1.2, Sr_1 =0.5, Sr_2 =1.0, S =3, and $\lambda = -0.5$.Therefore, the good comparison proves that bvp4c Matlab method is applicable to find subsequent results.

3. Results and Discussion

The solutions for ordinary differential equations together with the transformed boundary conditions are found using bvp4c function provided by the MATLAB software. The nature of the solutions obtained is dual. The numerical graphs are performed for three distinct increasing values of each governing parameters, namely Casson parameter β, Soret number for both components (Sr_1, Sr_2) and Soret number for both components (Db_1, Db_2). The highest boundary layer thickness

is set to be 30. The numerical results obtained are the profiles of velocity $f'(\eta)$, temperature $\theta(\eta)$, and concentration of component 1 $\phi_1(\eta)$ and component 2 $\phi_2(\eta)$.

Table 1
The list of physical parameters

Name of parameter	Mathematical formulation
Prandtl number	$\mathrm{Pr} = \frac{\nu}{\alpha}$
Buoyancy ratio of component 1	$N_{C1} = \frac{\beta_{C1}(C_{1w} - C_{1\infty})}{\beta_T(T_w - T_\infty)}$
Buoyancy ratio of component 2	$N_{C2} = \frac{\beta_{C2}(C_{2w} - C_{2\infty})}{\beta_T(T_w - T_\infty)}$
Radiation	$Rd = \frac{16\sigma^* T_\infty}{3kk^*}$
Thermophoresis	$Nt = \frac{\tau D_T(T_w - T_\infty)}{\alpha T_\infty}$
Modified Dufour parameters of component 1	$Db_1 = \frac{D_{TC1}(C_{1w} - C_{1\infty})}{\alpha(T_w - T_\infty)}$
Modified Dufour parameters of component 2	$Db_2 = \frac{D_{TC2}(C_{2w} - C_{2\infty})}{\alpha(T_w - T_\infty)}$
Lewis number of component 1	$Le_1 = \frac{\alpha}{D_{S1}}$
Lewis number of component 2	$Le_2 = \frac{\alpha}{D_{S2}}$
Soret number of component 1	$Sr_1 = \frac{D_{C1T}(T_w - T_\infty)}{D_{S1}(C_{1w} - C_{1\infty})}$
Soret number of component 2	$Sr_2 = \frac{D_{C2T}(T_w - T_\infty)}{D_{S2}(C_{2w} - C_{2\infty})}$
Suction	$S = \frac{v_w}{\frac{-3}{4}\alpha A^{1/4} x^{-1/4}}, \ S > 0$

Table 2
The comparison values to verified the current selected method

Formula	MatLab bvp4c	Shooting method
$f_{\eta\eta}(0)$	0.38029	0.38021
$-\theta_\eta(0)$	0.13150	0.13145
$-\phi_{1_\eta}(0)$	0.94024	0.94018
$-\phi_{2_\eta}(0)$	1.27354	1.27347

Dual numerical solutions are found in this study, namely as the first solution (solid line in the graphs) and second solution (dashed line in the graphs). However, only one solution is considered stable and physically reliable in the actual fluid situation. A stable solution is a graph without or with the minimum peaks because it fully satisfies the boundary conditions in Eq. (12) [8, 9, 17-21]. Therefore, the first solution is considered stable whereas another is recognized as the second solution in the Matlab bvp4c program.

The effects of β on the $f'(\eta)$ profile is displayed in Figure 2. This figure shows that when the increment of β reduces the first solution. Greater value of β will enhance the movement of molecules present in the fluid. This will make the molecules to collide with each other which slows down the fluid flow. Hence, $f'(\eta)$ in the stable solution deteriorates as value of β increases. However, the second solution shows that $f'(\eta)$ increases for low η but decreases for the higher η.

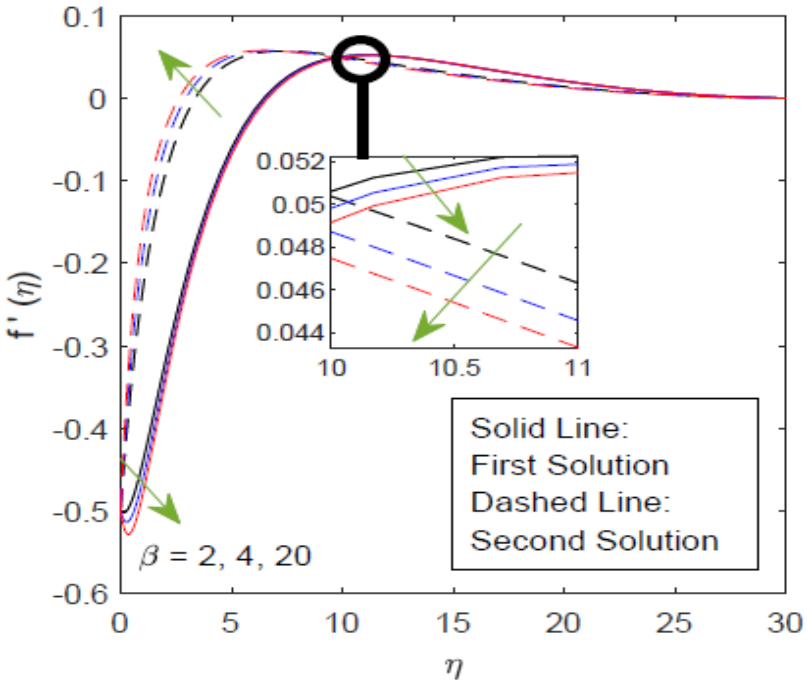

Fig. 2. The variation of $f'(0)$ against η for different values of β

Based on Figures 3 and 4, $\theta(\eta)$ profile behaves in opposite manner when the values of $(Sr_1,\ Sr_2)$ are increased. The first solution of $\theta(\eta)$ for various Sr_1(0.5, 0.6, 0.7) increases near the shrinking sheet. As the flow gets further from the shrinking sheet, the solution tends to fall until it reaches zero. The second solution falls for $0 \leq \eta \leq$30 as the value of Sr_1 increases. In contrast, the first solution initially falls when the value of Sr_2 increases, later the solution starts to rise for the range of η > 10. The $\theta(\eta)$ profile tends to rise and converges to zero when we increase the values of Sr_2 as 1.0, 1.02, 1.1 for the second solution. This behavior of $\theta(\eta)$ profile could be justified by the linear relationship between Sr_1 and Sr_2 and the difference of temperature near the sheet and away from the sheet. Thus, increment in these parameters induces the fluid flow to be hotter near sheet and less hotter when away from the shrinking sheet.

The Dufour number of component 1 and component 2 (Db_1, Db_2) also have some significant effects on the $\theta(\eta)$ profile as shown in Figures 5 and 6. Generally, the Dufour number of both components causes the temperature to rise for both first and second solution. The first solution for both increasing values of $Db_1$and Db_2 initially increases. Eventually, the solutions fall until it reaches zero as η approaches 30. The increment of Db_1 values rises the temperature in second solution for all the values of η. Whereas the second solution corresponding to Db_2 values decreases for larger value of η. The Dufour number is inversely proportional to the temperature difference. As the Dufour parameter is increased, the gradient between 2 positions (surface and ambient points) becomes smaller. This will make the temperature profile to increase. However at greater η, the profile decreases.

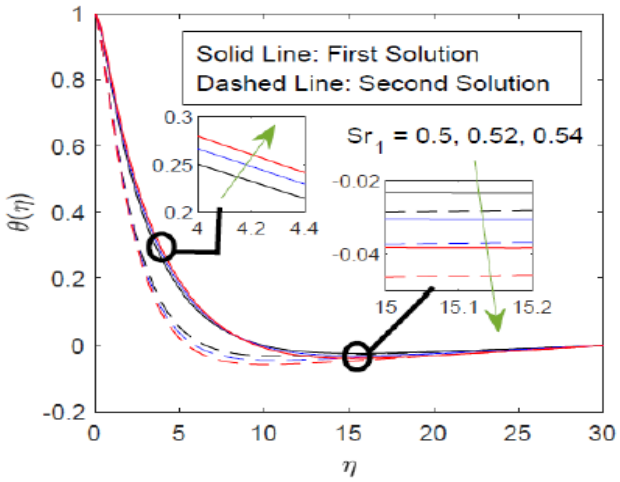

Fig. 3. The variation of $\theta(\eta)$ against η for different values of Sr_1

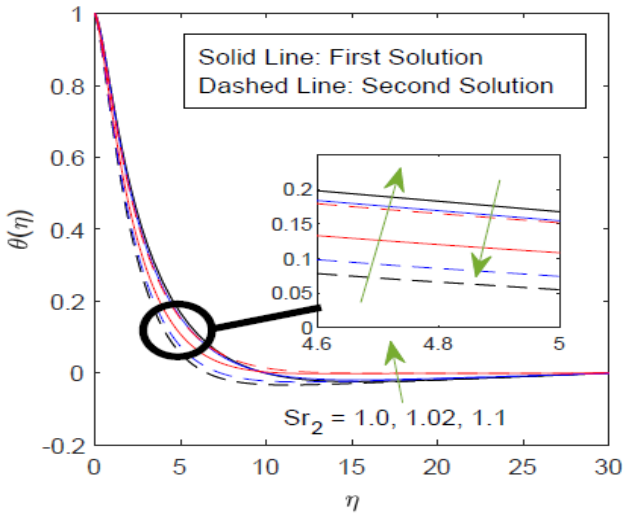

Fig. 4. The variation of $\theta(\eta)$ against η for different values of Sr_2

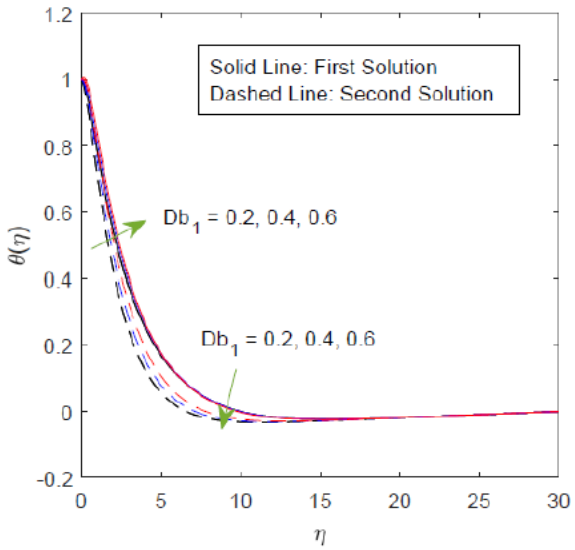

Fig. 5. The variation of $\theta(\eta)$ against η for different values of Db_1

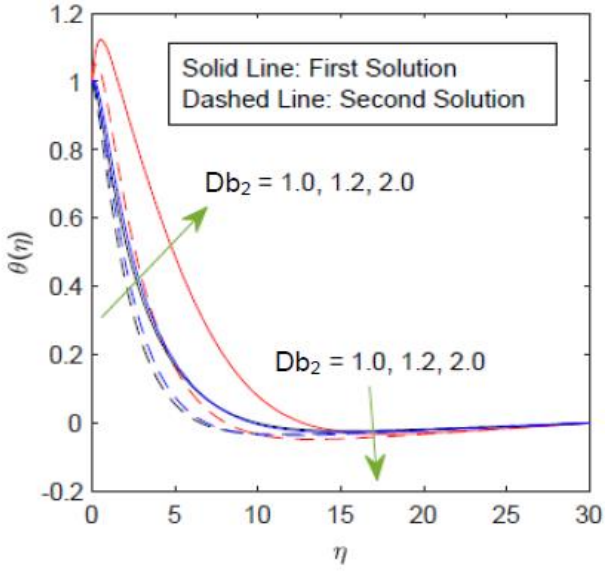

Fig. 6. The variation of $\theta(\eta)$ against η for different values of Db_2

It is also very vital to investigate the effects of Sr and Db parameters on concentration profiles of components 1 $\varphi_1(\eta)$ which saturate the Casson fluid as depicted in Figures 7 - 8. For increasing value of Soret and Dufour number, the first solution of component 1 concentration, $\varphi_1(\eta)$ behaves in only one manner. The concentration of component 1 increases as Sr_1 increases whereas it decreases as Db_1 increases. The second solution of $\varphi_1(\eta)$ profile behaves differently for smaller and larger range of η. The Soret number when increased, initially increases the concentration of component 1. When the value of η starts to get larger, component 1 become less concentrated as the rising Sr_1. The Dufour number causes the $\varphi_1(\eta)$ profile of component 1 to behave oppositely to that of Soret number. Initially the concentration decreases, later it starts to rise until it reaches 0.

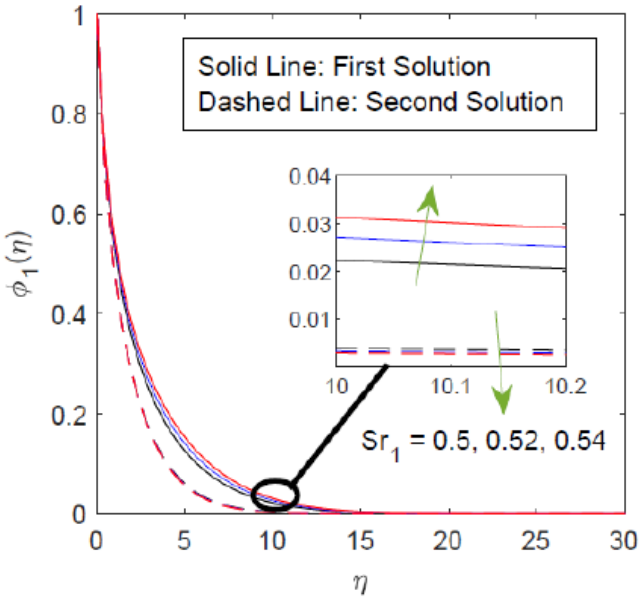

Fig. 7. The variation of $\varphi_1(\eta)$ against η for different values of Sr_1

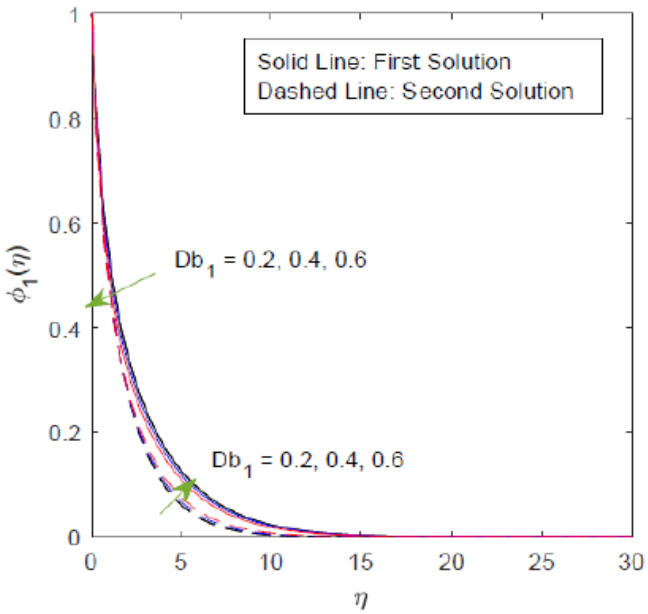

Fig. 8. The variation of $\varphi_1(\eta)$ against η for different values of Db_1

The graphs of concentration profile of component 2, $\varphi_2(\eta)$ against boundary layer thickness, η for various Sr and Db are illustrated in Figures 9 and 10, separately. It could be observed from Figure 9 that concentration decreases in the first solution for smaller range of . As the boundary layer becomes more thicker, the concentration starts to increase as the Soret number, Sr_2 is increased. The second solution of the profile possess a stable behavior. The value of $\varphi_2(\eta)$ increases as Sr_2 increases for $0 \leq \eta \leq 30$. Figure 10 depicts that increment in Dufour number, Db_2 causes the concentration profile of component 2 to vary in similar manner for both the solutions. To be precise, for smaller range of η, both solutions declines. When η become thicker, both the solutions rise back and approaches zero.

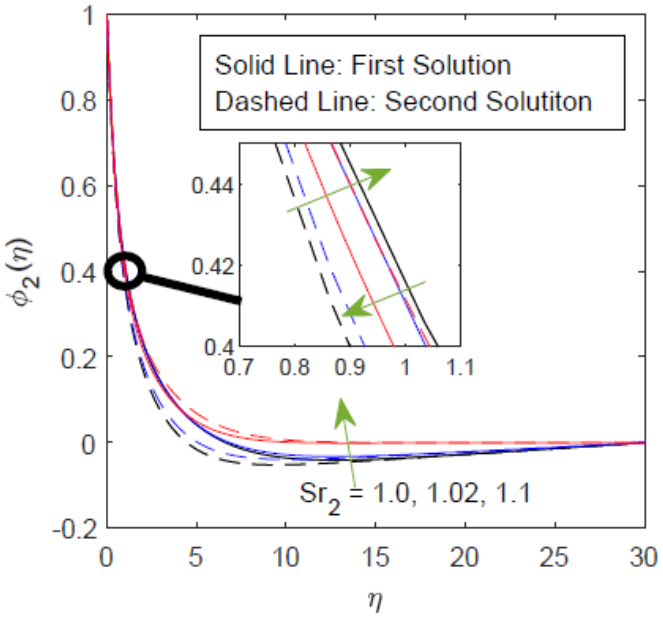

Fig. 9. The variation of $\varphi_2(\eta)$ against η for different values of Sr_2

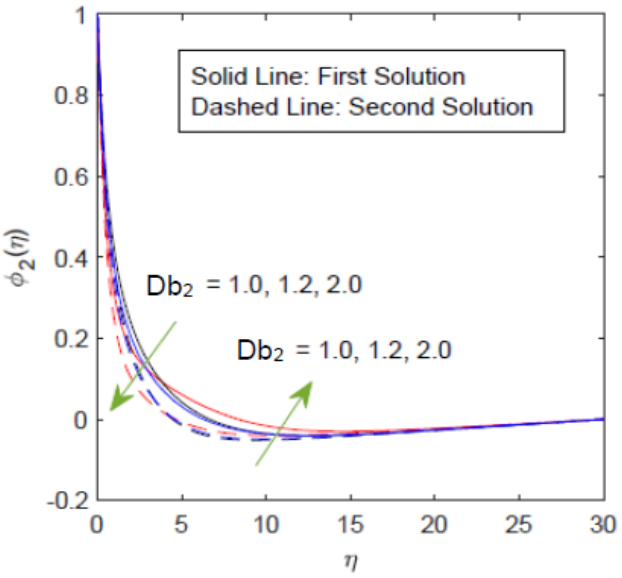

Fig. 10. The variation of $\varphi_2(\eta)$ against η for different values of Db_2

In general, the increment in Soret and Dufour parameters affects the concentration of component 1 and component 2 in opposite ways. Since Soret number displays an inverse relationship with the concentration difference of components, it could be verified that the Casson fluid becomes more concentrated due to the increasing Sr. Whereas, the scenery is totally different for Dufour parameter because it is directly proportional to concentration difference. Hence, any increment in this parameter will cause the components to become less concentrated. However, the components has greater concentration near the sheet compared to away from the sheet for both the parameters.

4. Conclusion

The triple-diffusive flow of non-Newtonian Casson fluid subjected to the Soret-Dufour effects have been solved by implemeting numerical approach (Matlab bvp4c program). Based on the findings which have been discussed in the previous section, the conclusions are listed as below:

i. Reducing the Casson parameter could accelerate The Casson fluid flow. This statement indicates that reducing the pseudo-plastic liquid characteristic causes the fluid to flow faster.
ii. If there is a need for the Casson fluid to be hotter for industrial purposes, then the Dufour parameter should be increased or Soret parameter should be decreased.
iii. An increment in Soret parameter makes the fluid to be more concentrated whereas an increment in Dufour parameter makes the fluid to be less concentrated as the sheet is compressed.

Finally, future research can be extended by developing the fluid flow model over different types of boundary shapes, such as cylinders, curved surfaces and thin needles. Moreover, Casson fluid could be a potential non-Newtonian fluid for future applications in science and technology.

Acknowledgement
The present research was funded by the Fundamental Research Grant Scheme (FRGS/1/2020/STG06/UPM/02/1) from the Ministry of Education (Malaysia)

References

[1] Pramanik, S. "Casson fluid flow and heat transfer past an exponentially porous stretching surface in presence of thermal radiation." *Ain Shams Engineering Journal* 5, no. 1 (2014): 205-212. https://doi.org/10.1016/j.asej.2013.05.003

[2] Satya Narayana, P. V., and B. Venkateswarlu. "Influence Of Variable Thermal Conductivity on Mhd Casson Fluid Flow Over a Stretching Sheet with Viscous Dissipation, Soret and Dufour Effects." *Frontiers in Heat and Mass Transfer (FHMT)* 7, no. 1 (2016). https://doi.org/10.5098/hmt.7.16

[3] Hayat, T., S. A. Shehzad, and A. Alsaedi. "Soret and Dufour effects on magnetohydrodynamic (MHD) flow of Casson fluid." *Applied Mathematics and Mechanics* 33 (2012): 1301-1312. https://doi.org/10.1007/s10483-012-1623-6

[4] Nadeem, Sohail, Rizwan Ul Haq, Noreen Sher Akbar, and Zafar Hayat Khan. "MHD three-dimensional Casson fluid flow past a porous linearly stretching sheet." *Alexandria Engineering Journal* 52, no. 4 (2013): 577-582. https://doi.org/10.1016/j.aej.2013.08.005

[5] Animasaun, I. L., E. A. Adebile, and A. I. Fagbade. "Casson fluid flow with variable thermo-physical property along exponentially stretching sheet with suction and exponentially decaying internal heat generation using the homotopy analysis method." *Journal of the Nigerian Mathematical Society* 35, no. 1 (2016): 1-17. https://doi.org/10.1016/j.jnnms.2015.02.001

[6] Bhattacharyya, Krishnendu. "MHD stagnation-point flow of Casson fluid and heat transfer over a stretching sheet with thermal radiation." *Journal of thermodynamics* 2013 (2013): 1-9. https://doi.org/10.1155/2013/169674

[7] Farooq, Umer, M. Ahsan Ijaz, M. Ijaz Khan, Siti Suzillianaa Putri Mohamed Isa, and Dian Chen Lu. "Modeling and non-similar analysis for Darcy-Forchheimer-Brinkman model of Casson fluid in a porous media." *International Communications in Heat and Mass Transfer* 119 (2020): 104955. https://doi.org/10.1016/j.icheatmasstransfer.2020.104955

[8] Parvin, Shahanaz, Siti Suzilliana Putri Mohamed Isa, Norihan Md Arifin, and Fadzilah Md Ali. "The magnetohydrodynamics Casson fluid flow, heat and mass transfer due to the presence of assisting flow and buoyancy ratio parameters." *CFD Letters* 12, no. 8 (2020): 64-75.

[9] Parvin, S., N. Balakrishnan, and S. S. P. M. Isa. "MHD Casson Fluid Flow Under the Temperature and Concentration Gradients." *Magnetohydrodynamics (0024-998X)* 57, no. 3 (2021). https://doi.org/10.22364/mhd.57.3.5

[10] Ahmad, K., S. S. P. M. Isa, Z. Wahid, and Z. Hanouf. "The Impact of Newtonian Heating on Magnetic Casson Nanofluid Flow with Variable Consistency Over a Variable Surface Thickness." *Magnetohydrodynamics (0024-998X)* 57, no. 3 (2021). https://doi.org/10.22364/mhd.57.3.1

[11] Al Oweidi, Khalid Fanoukh, Wasim Jamshed, B. Shankar Goud, Imran Ullah, Usman, Siti Suzilliana Putri Mohamed Isa, Sayed M. El Din, Kamel Guedri, and Refed Adnan Jaleel. "Partial differential equations modeling of thermal transportation in Casson nanofluid flow with arrhenius activation energy and irreversibility processes." *Scientific Reports* 12, no. 1 (2022): 20597. https://doi.org/10.1038/s41598-022-25010-x

[12] Yusof, Nur Syamila, Siti Khuzaimah Soid, Mohd Rijal Illias, Ahmad Sukri Abd Aziz, and Nor Ain Azeany Mohd Nasir. "Radiative Boundary Layer Flow of Casson Fluid Over an Exponentially Permeable Slippery Riga Plate with Viscous Dissipation." *Journal of Advanced Research in Applied Sciences and Engineering Technology* 21, no. 1 (2020): 41-51. https://doi.org/10.37934/araset.21.1.4151

[13] Kamis, Nur Ilyana, Noraihan Afiqah Rawi, Lim Yeou Jiann, Sharidan Shafie, and Mohd Rijal Ilias. "Thermal Characteristics of an Unsteady Hybrid Nano-Casson Fluid Passing Through a Stretching Thin-Film with Mass Transition." *Journal of Advanced Research in Fluid Mechanics and Thermal Sciences* 104, no. 2 (2023): 36-50. https://doi.org/10.37934/arfmts.104.2.3650

[14] Thirupathi, Gurrala, Kamatam Govardhan, and Ganji Narender. "Radiative magnetohydrodynamics Casson nanofluid flow and heat and mass transfer past on nonlinear stretching surface." *Journal of Advanced Research in Numerical Heat Transfer* 6, no. 1 (2021): 1-21.

[15] Roşca, Natalia C., Alin V. Roşca, and Ioan Pop. "Lie group symmetry method for MHD double-diffusive convection from a permeable vertical stretching/shrinking sheet." *Computers & mathematics with applications* 71, no. 8 (2016): 1679-1693. https://doi.org/10.1016/j.camwa.2016.03.006

[16] Patil, P. M., S. Roy, R. J. Moitsheki, and E. Momoniat. "Double diffusive flows over a stretching sheet of variable thickness with or without surface mass transfer." *Heat Transfer—Asian Research* 46, no. 8 (2017): 1087-1103. https://doi.org/10.1002/htj.21261

[17] Parvin, Shahanaz, Siti Suzilliana Putri Mohamed Isa, Norihan Md Arifin, and Fadzilah Md Ali. "Soret and Dufour effects on magneto-hydrodynamics Newtonian fluid flow beyond a stretching/shrinking sheet." *CFD Letters* 12, no. 8 (2020): 85-97. https://doi.org/10.37934/cfdl.12.8.8597

[18] Azmi, Hazirah Mohd, Siti Suzilliana Putri Mohamed Isa, and Norihan Md Arifin. "The boundary layer flow, heat and mass transfer beyond an exponentially stretching/shrinking inclined sheet." *CFD Letters* 12, no. 8 (2020): 98-107. https://doi.org/10.37934/cfdl.12.8.98107

[19] Parvin, S., S. S. P. M. Isa, and S. K. Soid. "Three-Dimensional Model of Double Diffusive Magnetohydrodynamic Newtonian Fluid Flow." *Magnetohydrodynamics (0024-998X)* 57, no. 3 (2021). https://doi.org/10.22364/mhd.57.3.6

[20] Parvin, Shahanaz, Siti Suzilliana Putri Mohamed Isa, Wasim Jamshed, Rabha W. Ibrahim, and Kottakkaran Sooppy Nisar. "Numerical treatment of 2D-Magneto double-diffusive convection flow of a Maxwell nanofluid: Heat transport case study." *Case Studies in Thermal Engineering* 28 (2021): 101383. https://doi.org/10.1016/j.csite.2021.101383

[21] Parvin, Shahanaz, Siti Suzilliana Putri Mohamed Isa, Fuad S. Al-Duais, Syed M. Hussain, Wasim Jamshed, Rabia Safdar, and Mohamed R. Eid. "The flow, thermal and mass properties of Soret-Dufour model of magnetized Maxwell nanofluid flow over a shrinkage inclined surface." *PLoS One* 17, no. 4 (2022): e0267148. https://doi.org/10.1371/journal.pone.0267148

[22] Patil, Prabhugouda Mallanagouda, and P. S. Hiremath. "Analysis of unsteady mixed convection triple diffusive transport phenomena." *International Journal of Numerical Methods for Heat & Fluid Flow* 29, no. 2 (2019): 773-789. https://doi.org/10.1108/HFF-04-2018-0134

[23] Rionero, Salvatore. "Triple diffusive convection in porous media." *Acta Mechanica* 224, no. 2 (2013): 447-458. https://doi.org/10.1007/s00707-012-0749-2

[24] Goyal, Mania, and Rama Bhargava. "Numerical study of thermodiffusion effects on boundary layer flow of nanofluids over a power law stretching sheet." *Microfluidics and nanofluidics* 17 (2014): 591-604. https://doi.org/10.1007/s10404-013-1326-2

[25] Archana, Manjappa, Bijjanal Jayanna Gireesha, and Ballajja Chandrappa Prasannakumara. "Triple diffusive flow of Casson nanofluid with buoyancy forces and nonlinear thermal radiation over a horizontal plate." *Archives of Thermodynamics* 40, no. 1 (2019): 49-69.

[26] Khan, Shahid, Mahmoud M. Selim, Aziz Khan, Asad Ullah, Thabet Abdeljawad, Ikramullah, Muhammad Ayaz, and Wali Khan Mashwani. "On the analysis of the non-Newtonian fluid flow past a stretching/shrinking permeable surface with heat and mass transfer." *Coatings* 11, no. 5 (2021): 566. https://doi.org/10.3390/coatings11050566

[27] Pop, Ioan, Siti Suzilliana Putri Mohamed Isa, Norihan M. Arifin, Roslinda Nazar, Norfifah Bachok, and Fadzilah M. Ali. "Unsteady viscous MHD flow over a permeable curved stretching/shrinking sheet." *International Journal of Numerical Methods for Heat & Fluid Flow* 26, no. 8 (2016): 2370-2392. https://doi.org/10.1108/HFF-07-2015-0301

[28] Isa, S. S. P. M., N. M. Arifin, R. Nazar, N. Bachok, F. M. Ali, and I. Pop. "MHD mixed convection boundary layer flow of a Casson fluid bounded by permeable shrinking sheet with exponential variation." *Scientia Iranica* 24, no. 2 (2017): 637-647. https://doi.org/10.24200/sci.2017.4048